Detection of ground states in frustrated molecular rings by in-field local magnetization profiles

M. Antkowiak, P. Kozłowski,* and G. Kamieniarz
Faculty of Physics, Adam Mickiewicz University, ul. Umultowska 85, 60-614 Poznań, Poland

G. A. Timco, F. Tuna, and R. E. P. Winpenny
School of Chemistry and Photon Science Institute, The University of Manchester, Manchester M13 9PL, United Kingdom
(Received 14 December 2012; revised manuscript received 23 April 2013; published 29 May 2013)

It is demonstrated by means of exact numerical methods that the ground state of nine-membered frustrated homometallic chromium-based molecular rings with a single bond defect can be unambiguously determined by the in-field local magnetization profiles, which exhibit characteristic patterns. The strength of the coupling corresponding to the defect can be determined by both total and local magnetization measurements on single crystals with the field perpendicular to the ring. This approach is illustrated with a recently synthesized chromium ring Cr_9Cl_2, which is experimentally characterized by low-temperature magnetic measurements and analyzed by means of the microscopic quantum model. The strength of the coupling corresponding to the defect is estimated by fitting the magnetic susceptibility of a powder sample and independently confirmed from the experimental intersection point of total magnetization profiles preserving the typical values of the remaining parameters, which are well established for known chromium rings.

DOI: 10.1103/PhysRevB.87.184430 PACS number(s): 75.50.Xx, 75.45.+j, 75.75.−c

I. INTRODUCTION

Molecular magnets have been recently intensively investigated in the hope to engineer a quantum computer[1–3] or an efficient information storage device,[4] and their role in the new field of spintronics[5–7] is constantly increasing. These materials are also very interesting from purely scientific point of view. Because of a well defined structure, a small size, and lack of intermolecular interactions between magnetic molecules, various quantum phenomena, such as, e.g., a discrete energy spectrum,[8] quantum tunneling of magnetization,[9,10] or Rabi oscillations[11] can be precisely detected and analyzed.

Both in pure and applied investigations, the determination of a quantum state of a molecule and its changes caused by external stimuli or by internal structure modification plays a crucial role. Thus finding unambiguous experimental manifestations of quantum states of a magnetic molecule may be very helpful in the precise determination of parameters in a model Hamiltonian or in selecting the right molecule for practical applications. However, such a process is usually long and expensive, requires the use of complex techniques,[12,13] and implies the necessity of making approximations and fitting the experimental data. Therefore it would be desired to develop a method that enables direct identification of quantum states and crucial microscopic parameters by means of simple measurements.

For the application in quantum computing, the minimum requirement is that a molecule is able to carry a qubit, i.e., the ground state of a molecule should be a doublet well separated from the lowest excited state. The most promising magnetic molecule having this property is the Cr_7Ni ring[14,15] in which the unfrustrated doublet ground state is generated by doping the homometallic Cr_8 ring with a Ni ion. However, like in an antiferromagnetic triangle,[16] a doublet ground state can also be obtained in odd-membered chromium-based antiferromagnetic rings[13,17] by the effect of geometric frustration.

In this paper, we address the problem of magnetic field driven identification of the quantum ground states and direct estimation of the single bond defect strength in the frustrated nine-membered $s = 3/2$ rings, which can have an $S = 1/2$ ground state and thus potentially can find application in quantum information processing. The approach is demonstrated for a recently synthesized molecular ring $[^i Pr_2NH_2][Cr_9F_9(O_2C^t Bu)_{17}Cl_2]$ (in short Cr_9Cl_2).

By fitting the magnetic measurements, it is shown that this molecule can be very well described by the model of a quantum spin ring with a single bond defect[17] and its behavior is characteristic of a second type of frustration.[13] We present numerical evidence that the measurements of total and local magnetization profiles in magnetic field can provide directly unambiguous information about ground states and the strength of the bond defect. All the theoretical calculations are performed by means of two accurate numerical methods: quantum transfer matrix (QTM) and exact diagonalization (ED).[18–22]

II. THE MOLECULE AND THE MODEL

The structure of Cr_9Cl_2 is presented in Fig. 1. The two (orange) chlorine ions replace one of two pivalic bridges connecting a chromium pair in the molecule and in this way make the bond defected, i.e., weaker than the remaining Cr-Cr bonds. The chemical synthesis is similar to that of other members of the Cr_9 family, which is described elsewhere.[13] Magnetic measurements have been performed on a Quantum Design MPMS-XL SQUID magnetometer. The magnetic susceptibility has been obtained in the dc magnetic field equal to 0.1 T.

It is assumed here that the spectroscopic and magnetic properties of the Cr_9Cl_2 molecule can be modeled by the Hamiltonian with a single bond defect:

$$\mathcal{H} = \sum_{j=1}^{8} J s_j \cdot s_{j+1} + \alpha J s_1 \cdot s_9 + \sum_{j=1}^{9} D\left(s_j^z\right)^2 - g\mu_B B \cdot \sum_{i=1}^{9} s_i, \quad (1)$$

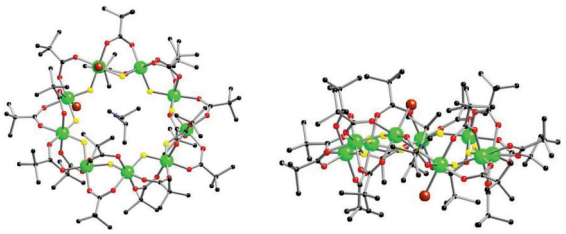

FIG. 1. (Color online) The structure of the Cr_9Cl_2 molecule. The colors (online) stand for the following ions: green Cr, yellow F, orange Cl, and red O. The rest of the structure is simplified.

where J and $J' = \alpha J$ stand for the exchange interactions between neighboring chromium ions, with the latter corresponding to the unique bond affected by the attached chloride ions; s_j stand for $s = 3/2$ spin operators and D is the single ion anisotropy. The coefficient α is referred to as the bond-defect parameter. If the magnetic field B is present, the Zeeman term enters the model (1) with the isotropic factor $g = 1.98$ and μ_B standing for Bohr magneton.

III. RESULTS

The model (1) has a symmetry with respect to the reflection in the plane perpendicular to the ring and intersecting its center and site 5. The exact eigenvectors conserve the total z component m of total spin and are invariant (symmetric) or change the sign (i.e., are antisymmetric) under the reflection operation. The eigenstates characterized by the value m are distinguished with respect to their transformation properties by the additional quantum number r equal to s or a, respectively. If no magnetic field is applied, the eigenvalues do not depend on the sign of m and are double degenerate, unless there is an accidental degeneracy, so that we can denote them by a quantum number $M = |m|$.

The exact ground-state phase diagram in α and D/J parameter space is sketched in Fig. 2. The states are characterized by the quantum numbers Mr. The boundary between the regions with the second (above) and the third (below) type of frustration is drawn by the continuous curve in Fig. 2 and defines the critical line $\alpha_c(D/J)$. The intersection of two energy levels corresponding to the ground states $1/2a$ and $1/2s$ at $\alpha = 1$ leads to the fourfold degeneracy characteristic of the first type of frustration. Here, we refer to the types of frustration proposed in Ref. 13.

In Fig. 2, the geometrically unfrustrated region spans below the horizontal dotted line $\alpha = 0$ and the region corresponding to the third type of frustration is located above this line and is limited from above by the solid line. The ground states $3/2s$ and $1/2s$ found in these regions come from the same $S = 3/2$ multiplet split by anisotropy.

In our accurate approach to the Cr_9Cl_2 molecule, the values

$$J/k_B = 16.6\ \text{K} \quad \text{and} \quad D/k_B = -0.34\ \text{K}$$

are fixed and taken from the INS and EPR experiments[12,23,24] on similar compounds of the Cr_8 family. Such a choice is motivated by the almost identical structure of the Cr-Cr bonds and by the similar geometry of the entire molecule. It has also led to good results in other works.[12,13] Possible small deviations from the values chosen above have minor influence

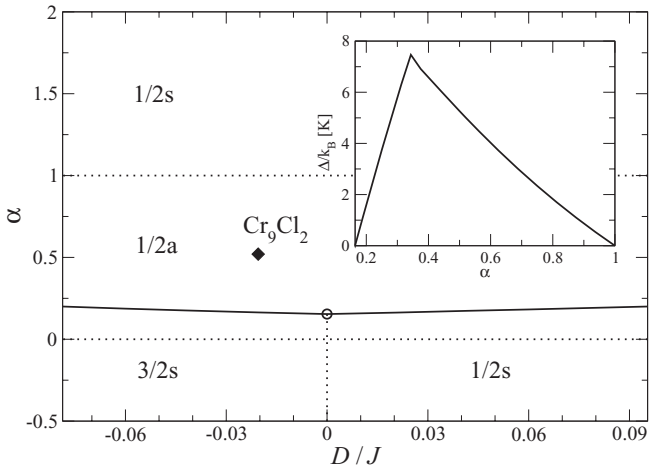

FIG. 2. $B = 0$ ground state as a function of anisotropy D/J and α. The diamond marks the coordinates of our theoretical fit for Cr_9Cl_2. The open circle represents a sixfold degenerated ground state, which appears at $\alpha_c = 0.154$. In the inset, the gap between the ground-state doublet $1/2a$ and the first excited state $3/2s$ or $1/2s$ is drawn as a function of α, for $D/J = -0.02$, which is the value obtained for Cr_9Cl_2.

on the results of our paper as exemplified by the influence of anisotropy D on the phase diagrams (see Figs. 2 and 4). By fitting the experimental susceptibility data presented in Fig. 3 with a small temperature independent correction (0.001 added to calculated susceptibility to account for temperature independent magnetism), the estimate of the bond-defect parameter is found and its value

$$\alpha = 0.52 \pm 0.02$$

is marked in Fig. 2. Cr_9Cl_2 system with $\alpha = 0.52$ is not bipartite and its behavior is affected by the second type of frustration.[13,25] Since the sample is polycrystalline, we had to take into account also transverse (with respect to anisotropy) components of susceptibility and magnetization, which could be calculated accurately only by means of the QTM technique. The details of this computational method can be found elsewhere[18–22] and its accuracy is demonstrated in Sec. IV.

The intersection point of the powder magnetization curves (see Fig. 3) is a witness to the $M = 1/2$ frustrated ground state since the powder magnetizations at this point attain a value close to 1, which is equal to gm. In Fig. 3, we also draw the theoretical single-crystal magnetization curves for various temperatures in the field applied along the z axis, which is perpendicular to the ring. These curves intersect each other at $B_i = 4.9$, i.e., in the middle of the first sharp magnetization step ($T = 0$), which ends at the critical field $B_{\text{cr}} = 9.81$ T. The theoretical estimate $B_i = 4.90$ T is in fact calculated as a limit (for $T \to 0$) of $b_i(T)$, defined as the intersection field of the magnetization calculated in temperature T and the magnetization in $T = 0$ (see the inset in Fig. 4). It agrees well with the experimental intersection point $B_{ex} = 4.6$ T corresponding in fact to the value of $b_i(T)$ for T between 2 and 4 K (inset in Fig. 4). We have checked that the relation

$$B_i = 1/2 B_{\text{cr}}$$

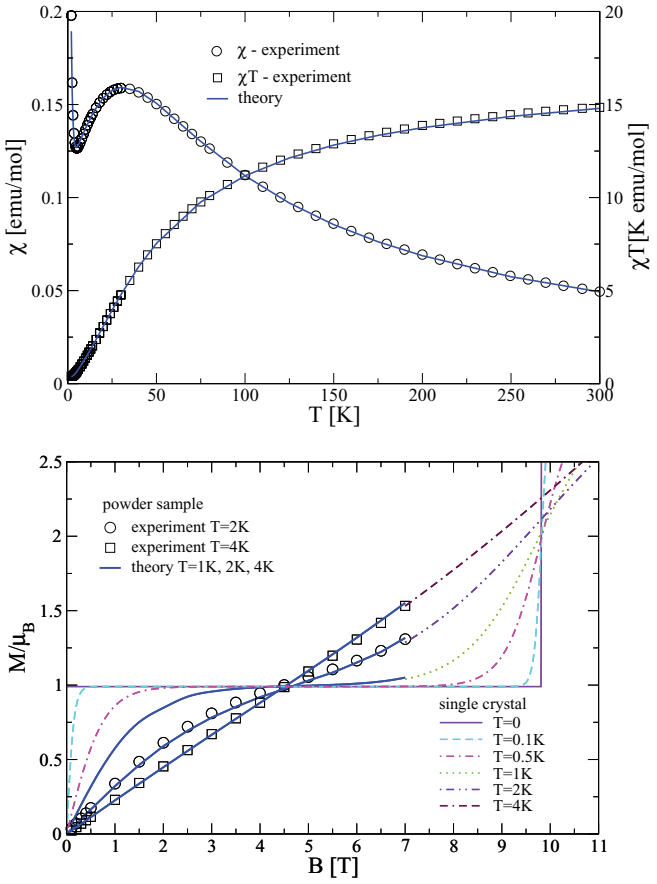

FIG. 3. (Color online) Powder susceptibility (top) and magnetization (bottom) as functions of temperature and magnetic field. The thick and thin lines represent the powder and single-crystal data, respectively.

is fulfilled also in the $3/2s$ phase and that the size of the step $B_{\rm cr}$ depends on α. The latter finding implies that given the theoretical dependence $B_{\rm cr}(\alpha)$, the bond defect parameter can be directly estimated from the experimental value of B_i. For the fixed value $D/J = -0.02$ corresponding to Cr_9Cl_2 (see Fig. 2), this crucial line $[B_{\rm cr}(\alpha)]$ separates the $1/2a$ and $3/2s$

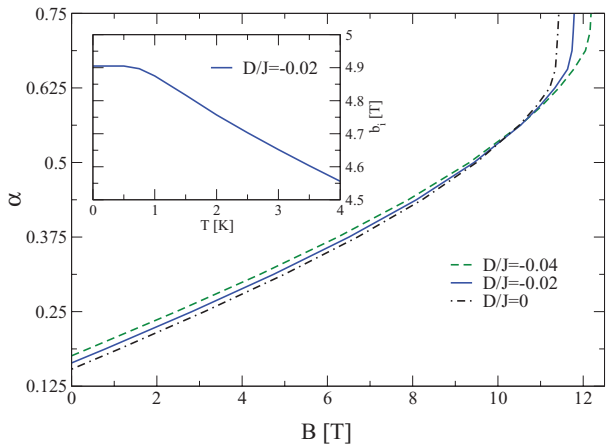

FIG. 4. (Color online) Critical line $B_{\rm cr}$ for three different ratios D/J. The inset presents convergence of $b_i(T)$ ($\alpha = 0.52$) in low temperatures.

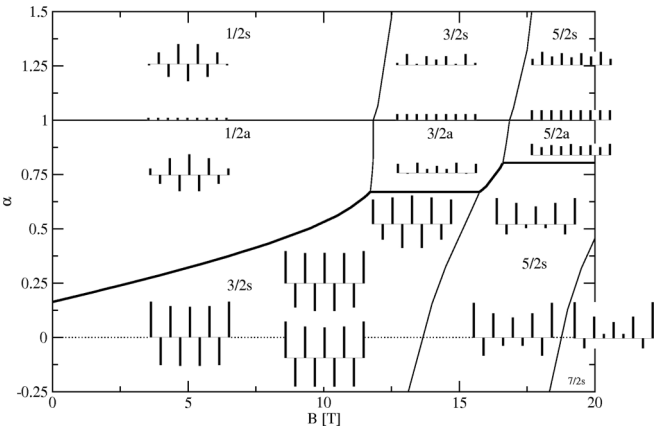

FIG. 5. Ground states Mr as a function of magnetic field B and α. The histograms embedded in the diagram represent local magnetization profiles.

phases in the diagram plotted in Fig. 5. Its precise position depends on the ratio D/J. Yet, for the values of D and J found in the literature on chromium rings,[26] this ratio variates roughly between -0.027 and -0.015. Thus leading to a very small variation of $B_{\rm cr}$ (see Fig. 4). As a result, the value of α can be estimated with a not worse precision than that attainable within the fitting procedure even if we assume some reasonable variation of the other parameters in Hamiltonian (1).

Though the critical lines separating the phases $1/2a$ and $3/2a$ as well as $1/2s$ and $3/2s$ are too steep to be used for determination of the parameter α from the total magnetization measurements they can be used at least to set the bounds for its value. Other critical lines (marked by solid lines in Fig. 5) separating various ground states induced by magnetic field and classified by quantum numbers Mr can also be used to determine the bond-defect parameter, given their dependence on α is strong enough and that one has in disposition a sufficiently strong magnetic field.

However, much more information can be provided by the local single-crystal magnetizations defined as

$$m_i = \langle s_i^z \rangle, \quad i = 1, \ldots, 9$$

with $\langle \cdots \rangle$ standing for thermal average.

The typical ground-state profiles of local magnetizations are sketched in Fig. 5 as a set of histograms. The external positions correspond to the sites 1 and 9 connected by the defected bond. The upper part of the pattern demonstrates the local spin components oriented along the field (applied in the zth direction) and the lower part—the spin components oriented in the opposite direction.

The data presented in Fig. 5 have been obtained by means of ED for $T = 0$. For a given phase and fixed α, the patterns do not change with increasing field [see Fig. 6(a)]. They change abruptly at the critical point and remain constant again. If the field is fixed and α is varied the local magnetizations change continuously within a given phase and abruptly at the phase boundaries (see Fig. 7). However, in the phases $1/2$s and $1/2$a, the signs and relations between local magnetizations (i.e., their sign and order) remain the same independent of particular values of α and B [see Fig. 7(a)]. Thus local magnetization patterns in these phases can be considered

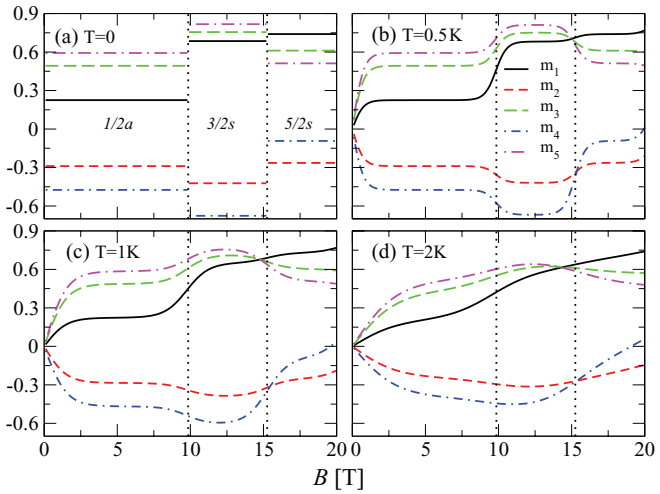

FIG. 6. (Color online) Local magnetizations for $\alpha = 0.52$ as a function of magnetic field B in four different temperatures $T = 0$, 0.5, 1, 2 T. Vertical doted lines separate different ground-state phases. The phases in (b)–(d) are the same as in (a). Due to the symmetry of the model, $m_1 = m_9$, $m_2 = m_8$, $m_3 = m_7$, $m_4 = m_6$.

universal and used to identify directly these two quantum states.

Within the other phases, the relative values of local magnetizations and/or their signs change, which can be seen in panels (b) and (c) of Fig. 7. For example, in Fig. 7(c) in the phase 5/2s, one can observe a change of sign of m_2 and m_4 and in panel (b) in both 3/2s phases there are intersections of local magnetization profiles. Thus, instead of one pattern, one can assign to each of these phases a set of few patterns characteristic for a given phase.

This method leads to unambiguous results given the measurement is done in sufficiently low temperature. At higher temperatures (above 0.5 K), the mixing of states due to thermal fluctuations leads to appearance of different patterns within a given phase even if α is fixed (see Fig. 6).

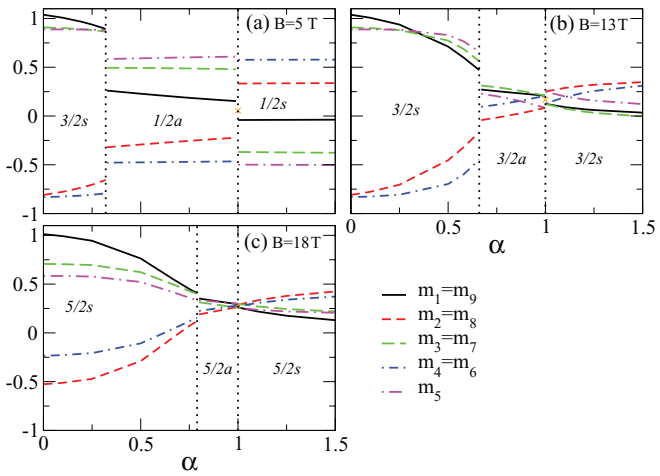

FIG. 7. (Color online) Local magnetizations at $T = 0$ as a function of α for three different fields $B = 5$, 13, 18 T. Vertical doted lines separate different ground-state phases.

Thus by measuring experimentally local magnetizations, one can directly determine the quantum state of a molecule. It is important to notice that what matters is the sign and the relative magnitude of local magnetization moments. Therefore even not very precise measurements can be used to determine unambiguously the quantum state of a frustrated molecule. This information cannot be inferred from the measurements of the total magnetization as there are different quantum states having the same total magnetization, e.g., 3/2s and 3/2a.

Besides, the local magnetization patterns provide also the estimates of the bond-defect parameter α and the coupling J' (if the value of J is known) since their change can be used to detect positions of critical lines in Fig. 5. The critical field B_{cr} along the transition line between the phases $1/2a$ and $3/2s$ gives directly the value of α whereas along the remaining transitions provides the bound for, e.g., if the transitions between the phases $1/2a$ and $3/2a$ or $1/2s$ and $3/2s$ are observed, the value of α can be then estimated as $0.671 \leqslant \alpha \leqslant 1$ or $\alpha \geqslant 1$, respectively.

IV. DISCUSSION

As it has been already mentioned, our theoretical results are numerically exact. Therefore we can account for the effect of anisotropy irrespective of its value. For magnetic field parallel to the anisotropy axis, Hamiltonian (1) is diagonalized without any approximation. For transverse field, ED is impossible (hard) due to the limited computer memory. Then, we use the QTM technique, which, though based on the Suzuki-Trotter formula, can provide results with arbitrary accuracy since we can reach the asymptotic quantum limit for any temperature considered in this paper. Figure 8 presents the convergence (with the Trotter index $m \to \infty$) of the QTM approximants calculated in transverse field to the exact values

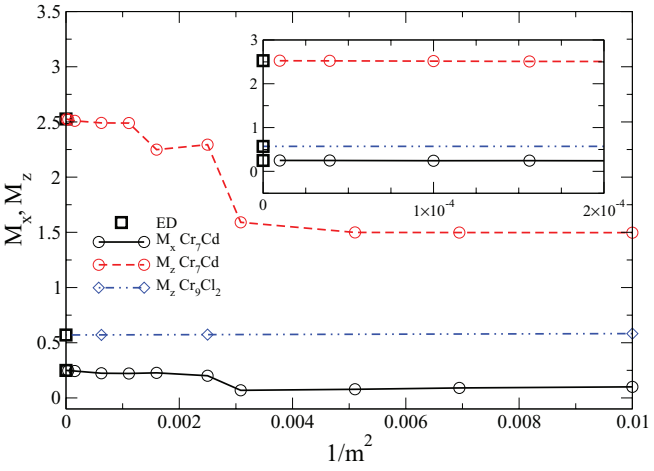

FIG. 8. (Color online) QTM approximants of the x and z projections of the total magnetization for Cr_7Cd ($J = 15.3$ K, $D = -0.31$ K, $T = 0.4$ K, $B = 20$ T, $\theta = 5.5°$) and Cr_9Cl_2 ($J = 16.6$ K, $\alpha = 0.52$, $D = -0.34$ K, $T = 2$ K, $B = 6$ T, $\theta = 0$) as a function of the Trotter index m. The magnetic field is applied in the x-z plane and forms the angle θ with the z axis, which is perpendicular to the ring. The inset represents the enlarged part of the main figure. The lines are drawn to guide the eye.

obtained by ED. These results of

$$M_x = \sum_{i=1}^{7} s_i^x \quad \text{and} \quad M_z = \sum_{i=1}^{7} s_i^z$$

were achieved for the model of a smaller system Cr_7Cd [corresponding to $\alpha = 0$ and the total number of spins equal to 7 in Hamiltonian (1)], for which ED is feasible also in the transverse field. In practice, it is enough to extrapolate the QTM results calculated for sufficiently large values of m since it is known[27] that then the QTM approximants depend linearly on $1/m^2$ (inset in Fig. 8). The particular value of m at which this asymptotic linearity appears depends on the calculated physical quantity, temperature, and the size of the system considered. For the Cr_9Cl_2 molecule, we found that for the lowest temperature accessible in the experiment, the asymptotic region begins already at the Trotter index $m = 10$ (see Fig. 8). Therefore we could safely extract all the thermodynamic quantities from the extrapolations obtained for $m > 10$, as in higher temperatures, the linear convergence is evident for even smaller values of m.

At this point, we would like to discuss the experimental verification and consequences of our findings. As to the experimental determination of the B_{cr} and the α values, it has been achieved here in the powder magnetization measurement because of the weak anisotropy ($D/J \sim 0.02$). The estimate $B_{ex} = 4.6$ T of B_i is found directly from the coordinates of the experimental intersection point in the lower panel of Fig. 3. This implies $B_{cr} = 9.2$ T and by referring to Fig. 5 one gets $\alpha \sim 0.49$ consistent with $\alpha = 0.52$ obtained from the fitting procedure. Using a higher magnetic field than in our experiment, the value of B_{cr} can be directly measured for $T = 1$ K (see the vicinity of the magnetization step in Fig. 3).

We emphasize that standard susceptibility and magnetization based fits may give ambiguous results. The proposed by us analysis of the magnetization intersection point and local magnetization histograms provides a new method to verify the correctness of the model parameters.

The idea of determining the ground states and the coupling of the defected bond by means of simple magnetic measurements can also be applied to other systems, e.g., Cr_8Ni, which has been analyzed within the fitting-based approach,[28] or to odd-membered systems of different size.

The local magnetizations can be observed experimentally. They were measured for the molecule Cr_7Cd in the NMR experiment[29] and for magnetic atoms adsorbed onto a nonmagnetic surface using spin-resolved scanning tunneling spectroscopy carried out up to 12 T.[30] All these mentioned above experimental techniques give sufficiently accurate results to be compared with the histograms calculated by us. The entire field range depicted in Fig. 5 is experimentally accessible.[31]

The compound Cr_7Cd is the ideal experimental realization of the geometrically unfrustrated ring with 7 spins and $\alpha = 0$. The profiles observed in Ref. 29 agree with those in Fig. 5 for $\alpha = 0$ and are nothing but the first experimental pattern revealing the $3/2s$ state.

Our patterns representing the quantum spin states are given for $T = 0$. As can be seen in Fig. 6, they remain practically unchanged in temperatures below $T = 0.5$ T except in the very close vicinity of the phase boundaries and $B = 0$.

The energy gap Δ between the ground-state doublet $1/2a$ and the first excited states ($3/2s$ for $\alpha \leqslant 0.343$ and $1/2s$ for $\alpha \geqslant 0.343$) depends on α and is plotted in the inset of Fig. 2 for $D/J = -0.02$. Its value for Cr_9Cl_2 ($\alpha = 0.52$) amounts to 5.01 K and is lower than that for the Cr_7Ni molecule ($\Delta/k_B \sim 13$ K).[14] The maximal magnitude of the energy gap $\Delta_{max}/k_B = 7.46$ K is obtained for $\alpha = 0.34$. We note that the almost maximal energy gap can be observed in a similar Cr_9F_{11} compound,[13] which can be modeled by the same Hamiltonian (1) and yields approximately $\alpha = 0.38$, which is close to the optimal $\alpha = 0.34$.

V. CONCLUSIONS

In conclusion, we have demonstrated that the local single-crystal magnetization profiles identify unambiguously the quantum ground states in the frustrated odd membered chromium ring with a single bond defect. Referring to the appropriate line in the numerically exact phase diagram (see Fig. 5), both these profiles and the infield total magnetization measurements provide also direct estimates of the coupling corresponding to the defected bond. Each of the phases 1/2s and 1/2a are characterized by only one pattern, whereas the remaining phases allow few different patterns.

We have characterized the Cr_9Cl_2 molecule as a ring with a single defected bond and have found its strength independently by fitting magnetic susceptibility and from the intersection point of the experimental magnetization profiles. As to the value $J = 16.60$ K of the coupling of the regular bonds, it was also a subject to modifications, which have not led to a better fit, however. The energy gap between the ground-state doublet and the first excited state is relatively small (5.01 K), which limits application of Cr_9Cl_2 in quantum computing. However, this gap can be increased to 7.46 K by proper chemical engineering of the molecule resulting in the weaker bond 1–9.

ACKNOWLEDGMENTS

One of us (G.K.) thanks M. Fardis for helpful discussions. We acknowledge the financial support from the national MNiSW Grant No. 230137. This work was granted access to the HPC resources in PSNC in Poznań and in the Academic Computer Center in Gdańsk (Poland) as well as those available within DECI programme by the PRACE-2IP under Grant No. RI-283493.

*kozl@amu.edu.pl

[1] M. N. Leuenberger and D. Loss, Nature (London) **410**, 789 (2001).
[2] J. Lehmann, A. Gaita-Ariño, E. Coronado, and D. Loss, Nat. Nanotechnology **2**, 312 (2007).
[3] G. A. Timco, S. Carretta, F. Troiani, F. Tuna, R. J. Pritchard, C. A. Muryn, E. J. L. McInnes, A. Ghirri, A. Candini, P. Santini, G. Amoretti, M. Affronte, and R. E. P. Winpenny, Nat. Nanotechnology **4**, 173 (2009).

[4]M. Mannini, F. Pineider, P. Sainctavit, C. Danieli, E. Otero, C. Sciancalepore, A. M. Talarico, M.-A. Arrio, A. Cornia, D. Gatteschi, and R. Sessoli, Nat. Mater. **8**, 194 (2009).
[5]S. Hill, R. S. Edwards, N. Aliaga-Alcalde, and G. Christou, Science **302**, 1015 (2003).
[6]M. Urdampilleta, S. Klyatskaya, J.-P. Cleuziou, M. Ruben, and W. Wernsdorfer, Nat. Mater. **10**, 502 (2011).
[7]R. Vincent, S. Klyatskaya, M. Ruben, W. Wernsdorfer, and F. Balestro, Nature (London) **488**, 357 (2012).
[8]M. L. Baker, T. Guidi, S. Carretta, J. Ollivier, H. Mutka, H. U. Güdel, G. a. Timco, E. J. L. McInnes, G. Amoretti, R. E. P. Winpenny, and P. Santini, Nat. Phys. **8**, 906 (2012).
[9]L. Thomas, F. Lionti, R. Ballou, D. Gatteschi, R. Sessoli, and B. Barbara, Nature (London) **383**, 145 (1996).
[10]M. Mannini, F. Pineider, C. Danieli, F. Totti, L. Sorace, P. Sainctavit, M.-a. Arrio, E. Otero, L. Joly, J. C. Cezar, A. Cornia, and R. Sessoli, Nature (London) **468**, 417 (2010).
[11]S. Bertaina, S. Gambarelli, T. Mitra, B. Tsukerblat, A. Müller, and B. Barbara, Nature (London) **453**, 203 (2008).
[12]S. Piligkos, H. Weihe, E. Bill, F. Neese, H. El Mkami, G. M. Smith, D. Collison, G. Rajaraman, G. A. Timco, R. E. P. Winpenny, and E. J. L. McInnes, Chem. Eur. J. **15**, 3152 (2009).
[13]M. L. Baker, G. Timco, S. Piligkos, J. S. Mathieson, H. Mutka, F. Tuna, P. Kozłowski, M. Antkowiak, T. Guidi, T. Gupta, H. Rath, R. J. Woolfson, G. Kamieniarz, R. G. Pritchard, H. Weihe, L. Cronin, G. Rajaraman, D. Collison, E. J. L. McInnes, and R. E. P. Winpenny, Proc. Natl. Acad. Sci. USA **109**, 19113 (2012).
[14]F. Troiani, A. Ghirri, M. Affronte, S. Carretta, P. Santini, G. Amoretti, S. Piligkos, G. Timco, and R. E. P. Winpenny, Phys. Rev. Lett. **94**, 207208 (2005).
[15]G. A. Timco, T. B. Faust, F. Tuna, and R. E. P. Winpenny, Chem. Soc. Rev. **40**, 3067 (2011).
[16]M. Luban, F. Borsa, S. Budko, P. Canfield, S. Jun, J. K. Jung, P. Kögerler, D. Mentrup, A. Müller, R. Modler, D. Procissi, B. J. Suh, and M. Torikachvili, Phys. Rev. B **66**, 054407 (2002).
[17]P. Kozłowski, M. Antkowiak, and G. Kamieniarz, J. Nanopart. Res. **13**, 6093 (2011).
[18]G. Kamieniarz, M. Bieliński, G. Szukowski, R. Szymczak, S. Dyeyev, and J.-P. Renard, Comput. Phys. Commun. **147**, 716 (2002).
[19]G. Kamieniarz, R. Matysiak, A. Caramico D'Auria, F. Esposito, and C. Benelli, Comput. Phys. Commun. **147**, 194 (2002).
[20]G. Kamieniarz and R. Matysiak, Comp. Mater. Sci. **28**, 353 (2003).
[21]G. Kamieniarz, P. Kozłowski, G. Musiał, W. Florek, M. Antkowiak, M. Haglauer, A. C. D'Auria, and F. Esposito, Inorg. Chim. Acta **361**, 3690 (2008).
[22]R. Matysiak, G. Kamieniarz, P. Gegenwart, and A. Ochiai, Phys. Rev. B **79**, 224413 (2009).
[23]S. Carretta, J. van Slageren, T. Guidi, E. Liviotti, C. Mondelli, D. Rovai, A. Cornia, A. L. Dearden, F. Carsughi, M. Affronte, C. D. Frost, R. E. P. Winpenny, D. Gatteschi, G. Amoretti, and R. Caciuffo, Phys. Rev. B **67**, 094405 (2003).
[24]R. Caciuffo, T. Guidi, G. Amoretti, S. Carretta, E. Liviotti, P. Santini, C. Mondelli, G. Timco, C. A. Muryn, and R. E. P. Winpenny, Phys. Rev. B **71**, 174407 (2005).
[25]J. Schnack, Dalton Trans. **39**, 4677 (2010).
[26]J. van Slageren, S. Piligkos, and F. Neese, Dalton Trans. **39**, 4999 (2010).
[27]M. Suzuki, Phys. Rev. B **31**, 2957 (1985).
[28]Y. Furukawa, K. Kiuchi, K. I. Kumagai, Y. Ajiro, Y. Narumi, M. Iwaki, K. Kindo, A. Bianchi, S. Carretta, P. Santini, F. Borsa, G. A. Timco, and R. E. P. Winpenny, Phys. Rev. B **79**, 134416 (2009).
[29]E. Micotti, Y. Furukawa, K. Kumagai, S. Carretta, A. Lascialfari, F. Borsa, G. A. Timco, and R. E. P. Winpenny, Phys. Rev. Lett. **97**, 267204 (2006).
[30]A. A. Khajetoorians, J. Wiebe, B. Chilian, S. Lounis, S. Blügel, and R. Wiesendanger, Nat. Phys. **8**, 497 (2012).
[31]S. Carretta, P. Santini, G. Amoretti, M. Affronte, A. Ghirri, I. Sheikin, S. Piligkos, G. Timco, and R. E. P. Winpenny, Phys. Rev. B **72**, 060403(R) (2005).